

# Strong broadband optical absorption in silicon nanowire films

Loucas Tsakalacos,<sup>a</sup> Joleyn Balch,<sup>a</sup> Jody Fronheiser,<sup>a</sup> Min-Yi Shih,<sup>a</sup>  
Steven F. LeBoeuf,<sup>a</sup> Mathew Pietrzykowski,<sup>a</sup> Peter J. Codella,<sup>a</sup> Bas A.  
Korevaar,<sup>a</sup> Oleg Sulima,<sup>b</sup> Jim Rand,<sup>b</sup> Anilkumar Davuluru,<sup>c</sup> and  
Umakant Rapol<sup>c</sup>

<sup>a</sup> General Electric - Global Research Center, Niskayuna, NY 12309, USA  
[tsakalacos@research.ge.com](mailto:tsakalacos@research.ge.com)

<sup>b</sup> GE Energy – Solar Technologies, Newark, DE 19702 USA

<sup>c</sup> General Electric - John F. Welch Technology Center, Bangalore, India.

**Abstract.** The broadband optical absorption properties of silicon nanowire (SiNW) films fabricated on glass substrates by wet etching and chemical vapor deposition (CVD) have been measured and found to be higher than solid thin films of equivalent thickness. The observed behavior is adequately explained by light scattering and light trapping though some of the observed absorption is due to a high density of surface states in the nanowire films, as evidenced by the partial reduction in high residual sub-bandgap absorption after hydrogen passivation. Finite difference time domain simulations show strong resonance within and between the nanowires in a vertically oriented array and describe the experimental absorption data well. These structures may be of interest in optical films and optoelectronic device applications.

**Keywords:** silicon, nanowire, optical properties, absorption, reflection, light trapping.

## 1 INTRODUCTION

Semiconducting nanowires have recently been the subject of great scientific and technological interest due to their promising electrical [1], optoelectronic [2], mechanical [3], and chemical properties [4]. High-mobility transistors [5], light emitting diodes [6], bio/chemical sensors [7], and other applications have been demonstrated primarily in the form of individual nanowire devices, though some devices based on arrays have been shown [8]. One aspect that has been generally overlooked is the interaction of light of varying wavelength with nanowire assemblies on a substrate, which may have implications for future optical and optoelectronic applications. The high aspect ratio of nanowires (typically on the order of 100 to 1000) and sharp dielectric contrast with its surrounding (e.g. air or glass) leads to optical anisotropy as observed in individual Si nanowires [9]. Moreover, sub-wavelength diameters and proximity, combined with micron scale lengths, may lead to interesting optical properties such as low reflectance and, as we show in this paper, high absorption.

Sub-wavelength resonance effects between nanowires are expected to produce a thin film with effective properties significantly different from a solid thin film. For example, ultra-low refractive index films based on SiO<sub>2</sub> nanowire arrays [10] as well as an optical antenna effect in carbon nanotube arrays [11] leading to reduced reflectance on Si substrates were recently demonstrated. Similar results have been shown for nanopatterned bulk Si substrates [12,13] and random nanostructured Si features [14,15].

It has been shown that high performance light trapping schemes have the potential to enhance the short-circuit photocurrent, and therefore efficiency, in various solar cells, including silicon-based single and multi-junction thin film solar cells by as much as 25% [16]. This is particularly true for microcrystalline Si, where enhancements in the 600-1000 nm range are desired. Furthermore, random microstructures induced by laser-treatment have also

been shown to improve the near-infrared performance of silicon avalanche photodetectors [17].

Here we demonstrate, by fabricating Si nanowire films on glass substrates, that both their optical reflection and transmission characteristics are significantly modified compared to solid films across the spectral range of 300-2000 nm. We show the observed behavior is due to strong light trapping within the nanowire films, combined with strong defect state absorption as observed in the sub-bandgap spectra.

## 2 EXPERIMENTAL DETAILS

Silicon nanowires films were fabricated/synthesized directly on fused SiO<sub>2</sub> or soda-lime glass substrates to allow measurement of both total reflection and total transmission through the nanowire arrays. Two types of samples were studied: Type A samples were fabricated by anodic bonding of a 300 μm thick silicon wafer (<100>-oriented, phosphorus doped, ρ = 0.5 Ω-cm) to soda-lime glass wafers. The Si wafer was then coated with a Si<sub>x</sub>N<sub>y</sub> thin film (thickness = 200 nm) deposited by low-pressure chemical vapor deposition (LPCVD). Photolithography combined with RIE was used to delineate a 1" diameter hole in the silicon nitride film, which allowed wet etching of the bulk Si in KOH to a thickness of 1-40 μm. Samples with a total thickness of ~11 μm are reported here, though similar effects are observed for films as thin as 1 micron. Nanowires were then formed using a galvanic wet etching process in a Ag nitrate:HF bath at room temperature, producing vertically oriented nanowires (Fig. 1a) [18]. While individual nanowires with diameters in the range of 5-10 nm have been observed, typically they are larger (20-100 nm) or bundled together as a result of the drying process. The length of the nanowires can be controlled from 1 to 40 μm by adjusting the wet etching time. It was not possible to create a film consisting only of nanowires due to adhesion problems; therefore the Type A samples typically consisted of a thick nanowire array (i.e. 2-40 μm) on top of a thin solid Si thin film (i.e. ~0.5-1 μm) in contact with the glass substrate (Fig. 1a).

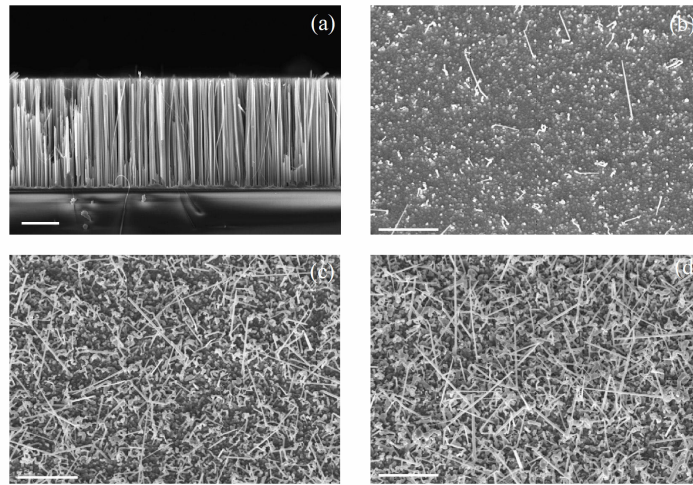


Fig. 1. (a) Cross-sectional SEM image of a 10 micron thick nanowire array (type A) on glass substrate with an ~1 micron thick solid Si intermediate layer, and SEM images (taken at 30° tilt) of Type B samples grown with a catalyst thickness of (b) 10 Å, (c) 25 Å, (d) 50 Å. The length of all micron markers in these images is 4 microns.

Type B samples were formed on fused silica substrates by first electron-beam evaporating (at room temperature) a thin Au layer of varying thickness (10, 25, and 50 Å) on the substrate. Nanowires were synthesized using the vapor-liquid-solid (VLS) growth mechanism [19] in a hot-wall chemical vapor deposition (CVD) system at 560°C using a 1:6 mixture (20 sccm and 5 sccm, total pressure ~ 0.5 Torr) of silane and hydrogen flowing for 30 minutes (Figure 1b-d). The samples were characterized using scanning electron microscopy (LEO 1530 VP field emission SEM).

Transmission (T) and reflectance (R) spectra were obtained on a Cary 5000 UV/Vis/NIR spectrophotometer employing deuterium and mercury lamps, and equipped with a 150 mm integrating sphere. Total optical reflectance was obtained by illuminating the sample at 8° off-normal and integrating the specular and diffuse reflectance. Reflectance spectra were referenced to Spectralon standards (Labsphere Inc., North Sutton, NH). Total transmission was obtained by placing the sample over the opening of the integrating sphere and illuminating with normal, monochromatic light. Transmission measurements were referenced to the beam entering the open integrating sphere. The effective absorption (A) in the films was defined as  $A = 1 - T - R$  without any correction for thin film effects or other possible losses, since comparisons of samples on the same types of transparent substrate were made.

### 3 RESULTS AND DISCUSSION

Figure 2a shows typical total optical reflectance spectra of Type A samples and of an 11 μm thick solid film (acting as a control) that was thinned by KOH etching (no attempt to polish was made). The reflectance of the solid film shows typical behavior expected for silicon, whereas the reflectance of the nanowire film is less than 5% over the majority of the spectrum from the UV to the near IR and begins to increase at ~700 nm to a values of ~41% at the Si band edge (1100 nm), similar to the solid film sample. We note that the solid Si film reflectance begins to increase slightly at ~ 800 nm, rather than at ~1,000 nm, due to the fact that there is more loss of back-reflected long wavelength light from the top surface for such a film compared to a bulk substrate, and the fact that as fabricated solid Si films are slightly textured (i.e. it is rough at the micron scale). Therefore, our solid film data cannot be directly compared to bulk, polished Si optical properties. Nevertheless, it is clear that the nanowires impart a significant reduction of the reflectance compared to the solid film. It is also noteworthy that the spectral dependence and magnitude of the total reflectance for our samples are much improved compared to those found in the literature. For example, Rappich *et al.* [20] obtained reflectance values for nanoporous silicon ranging from ~2-30 % and ~2-20%

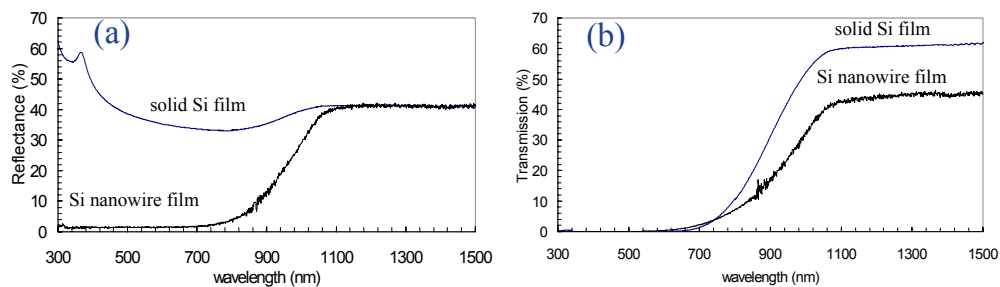


Fig. 2. (a) Total reflectance data from integrated sphere measurements for an 11 μm thick solid Si thin film and Type A nanowire film on glass substrate; (b) total transmission data for solid thin film and Type A nanowire film on glass substrate.

in anodized nanowire-like structures in the 300-850 nm wavelength range. By comparison, in the same wavelength range our samples typically show a constant total reflectance of  $\leq 2\%$  and a specular reflectance of  $< 1\%$  (not shown), on par with recent data presented by Shubert and co-workers for graded index nanostructured films [21]. In some samples we observe oscillations in the nanowire film total reflectance spectrum and in others this is not observed. This is related to the thickness and uniformity of the residual film layer beneath the nanowires, which can vary from sample to sample, leading to interference effects.

More striking is the fact that the transmission of the nanowire samples is also significantly reduced for wavelengths greater than  $\sim 700$  nm (Figure 2b). This implies that there is strong absorption occurring within the nanowire layer, for example, due to significant light trapping. The absorption curves in Figure 3, derived from transmission and reflectance data such as in Figure 2, also shows there is strong residual absorption below the Si bandgap for the Si nanowires. Because the nanowires are homogeneously composed of single-crystal

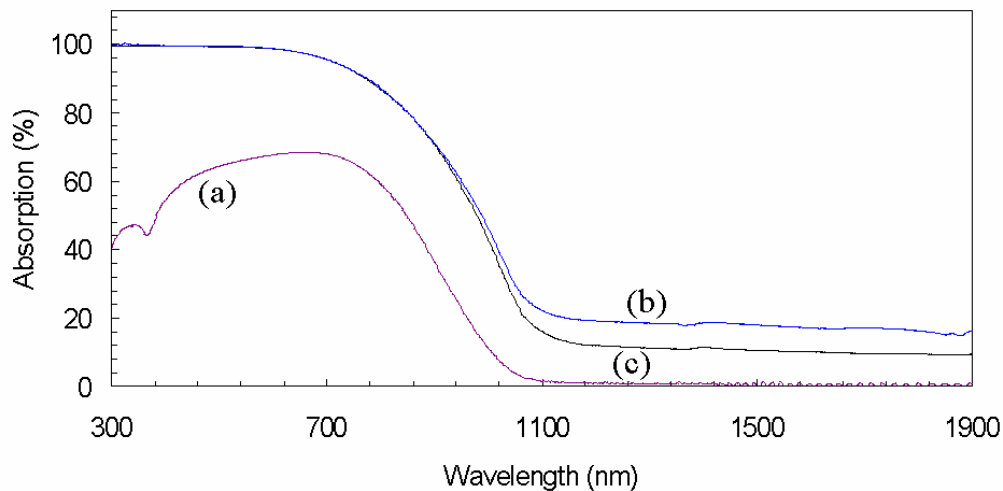


Fig. 3. Absorption data (calculated from T and R data similar to that in figure 2) for (a) solid Si film, (b) Type A etched nanowire film on glass, (c) the same Type A etched nanowire film on glass after annealing in forming gas showing reduced below bandgap absorption.

silicon, this residual absorption is attributed to strong IR light trapping coupled with the presence of surface states on the nanowires that absorb below bandgap light. Surface states are known to occur in porous Si due to the etch process and have a strong impact on the optical properties [22] and to contribute to sub-bandgap absorption in microstructured Si [23]. Indeed, after we annealed samples in forming gas for 30 min at  $400^{\circ}\text{C}$  the optical absorption below the bandgap was found to decrease, indicating that surface states might be partially responsible for this sub-gap absorption as they were partially passivated (Figure 3). As will be clear from the discussion below, this sub-bandgap absorption is a result of light trapping such that on multiple interaction with the nanostructured layer, the light is absorbed on each pass by such surface states and related defects. The level of optical absorption below  $\sim 800$  nm does not change with passivation, which further indicates that light trapping plays a dominant role in the enhanced absorption of the structures at all wavelengths (since the medium becomes absorbing above the bandgap, see below). Similar curves as in Figure 3 have been obtained for Type A nanowire arrays with lengths down to  $\sim 1\mu\text{m}$ . It is not possible to control the wet etch process to yield uniform nanowire with a length below this value.

Polarization-angle dependent and angle-resolved specular reflectance measurements (up to 70 degrees from substrate normal) on the vertically well-aligned Type A samples were also attempted to elucidate the effect of polarization in such high aspect ratio structures. However,

due to the extremely low specular reflectance for such samples (below 1%) such measurements were inconclusive. The extremely low specular reflectance is indeed maintained up to high angles. The Type A nanowire film samples generally look black or dark brown at all observation angles, making them useful for various optoelectronic applications, e.g. in photo-detectors, solar cells, etc.

We also studied the optical properties of CVD grown Si nanowire films on glass (Type B samples, Figure 4). In this case the nanowires are not oriented and heterogeneously nucleate on top of a nanocrystalline phase separated Au-Si composite film (~100 nm thick), with the nanowire density increasing with larger catalyst film thickness. In addition to the well-known presence of a catalyst nanoparticle on the top of each nanowire, the nanowires also typically contain small Au nanoparticles on the surface under our growth conditions. As in the case of the wet etched nanowires (type A), the nanowire film shows significantly stronger absorption across the spectrum for nanowires grown on a catalyst thickness of 25 Å or greater, with the sub-bandgap absorption being higher than that of the etched wires and gradually decreasing with increasing wavelength. Control samples with a Au thin film before and after annealing at the same temperatures as the CVD growth (to form Au nano-islands) do not show this effect, i.e. the absorption above 1000 nm is less than 5%, though a single, broad peak at shorter wavelengths characteristic of plasmon resonance was observed.

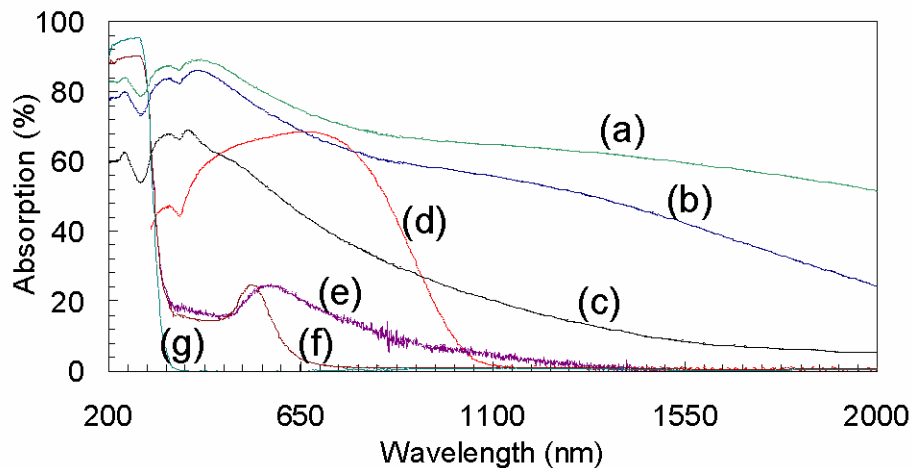


Fig. 4. Optical absorption data for Type B nanowire samples grown using a catalyst thickness of (a) 50 Å, (b) 25 Å, and (c) 10 Å showing enhanced absorption of the nanowire samples compared to (d) a Si solid film (same data as in Fig. 3); Absorption data for a 50 Å thick Au film on glass (e) before and (f) after thermal annealing at the same temperature and time as the nanowire growth (though without silane flow); and (g) absorption data for a bare glass substrate. We have observed a similar increasing trend in absorption with nanowire growth time for a fixed catalyst thickness.

As noted above, the observed behavior is associated with strong light trapping in the nanowire arrays. Light trapping is typically defined as the ratio of the effective path length for light rays confined within a structure with respect to its thickness. Yablonovitch and Cody [24] showed by statistical mechanical arguments that for a randomly or regularly textured surface on a non-absorbing medium, the effective path length is given by  $2n^2$ , which for silicon implies an optical path length of between 20 and 65 depending on the wavelength. For an absorbing medium the absorption enhancement is on the order of  $4n^2$ . In the case of our nanowire arrays, the thickness (length of the wires) is generally greater than the optical absorption depth; therefore an effective refractive index based on the volume fraction of nanowires must be utilized. Nevertheless, it is reasonable to ask if any additional physics is operable in the measured nanowire array absorption behavior.

The above results may be explained using two potential theoretical frameworks: 1) antenna theory, and 2) Mie scattering theory. Y. Wang et al. [11] described length dependent, polarized reflectance data from carbon nanotube arrays as arising from an antenna effect in the nanotubes. While such effects are possible in Si nanowire films, length dependent reflectance data on bulk Si substrates (not shown) did not yield any well-defined reflectance peaks, suggesting our Si nanowires are not efficient antenna elements. The orders of magnitude higher electrical resistivity of Si compared to CNTs and long nanowire lengths compared to the CNT samples reported by Wang et al. [11] makes our Si nanowire films poor antenna elements, ruling out antenna theory as an effective means of describing the observed phenomena. Alternatively, the theory associated with sub-wavelength scattering, i.e. Mie theory that is closely related to the so called “moth-eye effect” [25], is more relevant to the structures described here and is well described by an effective medium theory [26]. Indeed, Mie scattering theory along with Lambertian light trapping has been successfully used to model the optical absorption enhancement of silicon films containing spherical voids [27].

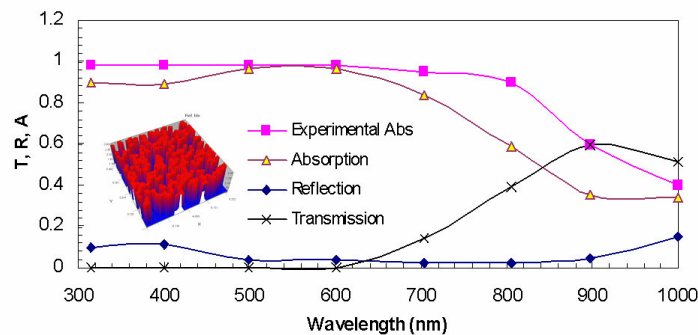


Fig. 5. FDTD model (Optiwave, Inc.) of randomly placed 10 micron long silicon nanowires on a 1 micron thick bulk substrate. Reflection, transmission, and absorption curves derived from such a model showing generally good agreement with data presented in this work. The nanowire area fraction was 0.18 in the model and  $\sim 0.4$  in the experimental sample. The lines are meant to guide the eye. We note that when the model is extended beyond 1,100 nm a residual effective absorption is observed due to interference effects.

In order to begin to understand how light interacts with the sub-wavelength vertically aligned (Type A) nanowire arrays, we have performed modeling studies of individual and arrays of nanowires using finite difference time domain methods [28] (Optiwave, Inc.) that clearly show that collective optical resonances between nanowires may occur in such arrays (Figure 5). In our model we input wavelength-dependent  $n$  and  $k$  values for Si obtained from the literature. The calculated absorption spectra were obtained with standard optics, either a single nanowire diameter or a distribution of diameters (as is expected experimentally), and without assuming any surface states. The model size ranged from 1.6 by 1.6 microns to 10 by 10 microns with nanowires 2-10 microns in length on top of a 1 micron thick solid Si film. The modeled absorption spectra in Figure 5 show good agreement with experimental data, even though the area fractions for the two were somewhat different. Indeed, we varied the nanowire area fraction from 0.1 to 0.84. As expected, the absorption at a given wavelength was the same in the limit of low and high-density nanowires, with a broad peak at intermediate nanowire densities (Figure 6). Our calculations also show that the absorption edge of a nanowire films shifts to longer wavelengths and approaches the bulk value as the nanowire density is increased. Essentially, the Si nanowire arrays act as sub-wavelength cylindrical scattering elements, with the macroscopic optical properties being dependent on nanowire pitch, length, and diameter.

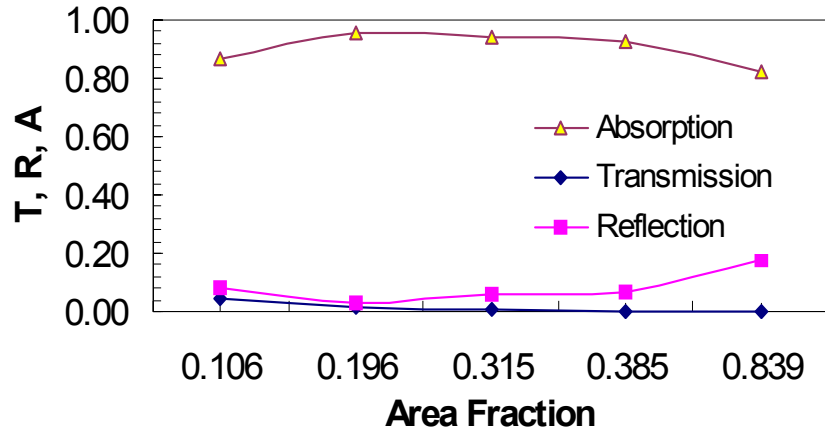


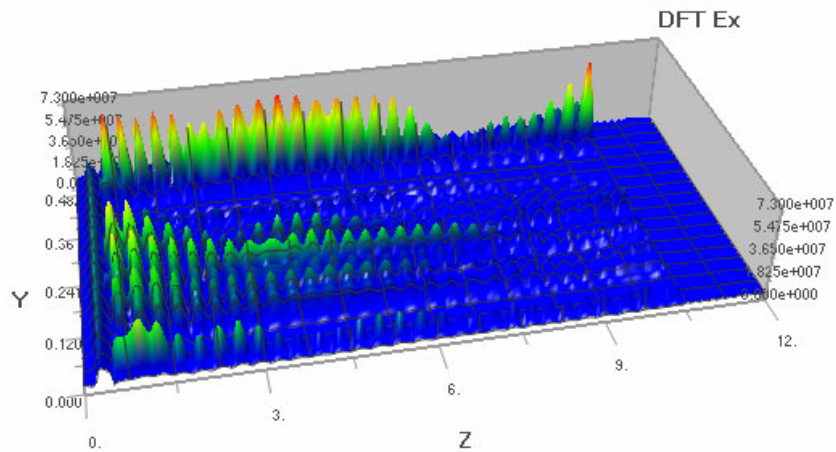
Fig. 6. Nanowire area fraction dependence of absorptions, transmission, and reflectance at  $\lambda = 500$  nm and a nanowire diameter of 50 nm. The nanowires were modeled on top of a 1 micron thick solid Si substrate.

Furthermore, our calculations show that diameter dependent Mie-type scattering [29] and absorption occur within each wire (data not shown), though the wires may be viewed as infinite cylinders within the context of Mie theory. Figure 7 shows a snapshot of the transverse component of the light interacting with the nanowire elements. It is clear that resonance between the wires and within the wires occurs, which supports the notion of strong light trapping.

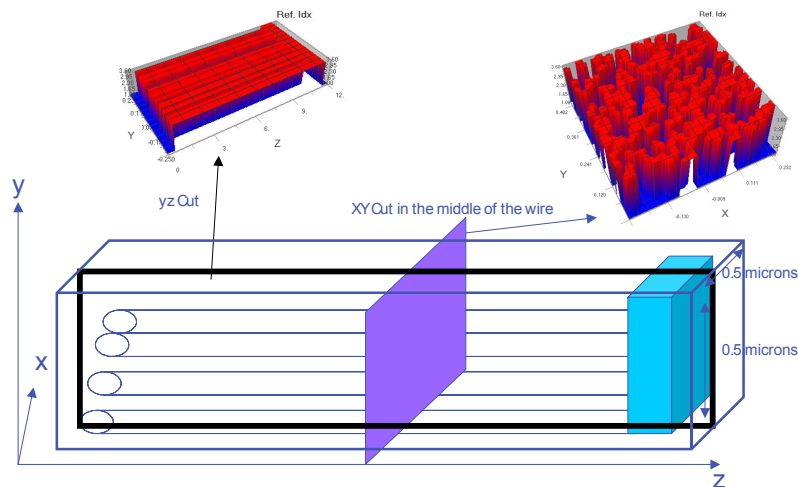
Finally, while the high sub-bandgap absorption may be explained by light trapping coupled with strong absorption by point, line, and planar defect states [23], it is plausible that part of the enhanced absorption behavior in the Type B nanowires films is due to the plasmon coupling of light with the nanowires and underlying nanocrystalline film, particularly since the area density of nanowires in the film is relatively low compared to the Type A samples. Plasmon coupling has recently been shown to contribute to the optical properties of CdS-Au nanoparticle complexes [30] and the use of plasmonic nanoparticles with a distribution of diameters has been studied theoretically for broadband capture of the solar spectrum [31]. Further experiments and modeling are required to clarify the effect of the random orientation of the nanowires, and the possible effect of plasmonic coupling in the underlying film and on the nanowires.

#### 4 CONCLUSIONS

In conclusion, we have demonstrated that Si nanowire films possess unique macroscopic optical properties. The nanowires yield significantly reduced optical reflection over the full spectrum above the bandgap, as well as reduced transmission for wavelengths greater than  $\sim 700$  nm in the case of  $\sim 10$   $\mu\text{m}$  long wires. The strong residual absorption below the bandgap is shown to be due to a combination of etching induced surface states, which can be reduced after a hydrogen passivation annealing step, and significant light trapping within the nanowire film.



(a)



(b)

Fig. 7. (a) Snapshot of the electric field component ( $E_x$ ) of an electromagnetic plane wave ( $\lambda = 1,107$  nm) propagating through (b) a 0.5 by 0.5 micron nanowire array (30 nm diameter, 10  $\mu$ m long wires) showing scattering and resonance of light within the structure. The field of view is taken such that the length of the nanowires is along the Z direction (in the YZ plane) and the plane wave is launched from left to right along the z axis.

### Acknowledgments

The authors thank the GE Nanotechnology Program (M.L. Blohm) for financial support of this work. The experimental assistance from and useful discussions with R. Wortman, A. Brinton and S. Kennerly are appreciated by the authors.

## References

- [1] G. Zheng, W. Lu, S. Jin, and C. M. Lieber, "Synthesis and fabrication of high-performance n-type silicon nanowire transistors," *Adv. Mater.* **16**(21), 1890-1893 (2004) [[doi:10.1002/adma.200400472](https://doi.org/10.1002/adma.200400472)].
- [2] F. Qian, Y. Li, S. Gradecak, D. Wang, C. J. Barrelet, and C. M. Lieber, "Gallium nitride-based nanowire radial heterostructures for nanophotonics," *Nano. Lett.* **4**(10), 1975-1979 (2004) [[doi:10.1021/nl0487774](https://doi.org/10.1021/nl0487774)].
- [3] C. Y. Nam, P. Jaroenapibal, D. Tham, D. E. Luzzi, S. Evoy, and J. E. Fischer, "Diameter-dependent electromechanical properties of GaN nanowires," *Nano. Lett.* **6**(2), 153-158 (2006) [[doi:10.1021/nl051860m](https://doi.org/10.1021/nl051860m)].
- [4] Y. Zhang, A. Kolmakov, S. Chretien, H. Metiu, and M. Moskovits, "Control of catalytic reactions at the surface of a metal oxide nanowire by manipulating electron density inside it," *Nan. Lett.* **4**(3), 403-407 (2004) [[doi:10.1021/nl034968f](https://doi.org/10.1021/nl034968f)].
- [5] Y. Cui, Z. Zhong, D. Wang, W. U. Wang, and C. M. Lieber, "High performance silicon nanowire field effect transistors," *Nan. Lett.* **3**(2), 149-152 (2003) [[doi:10.1021/nl0258751](https://doi.org/10.1021/nl0258751)].
- [6] Y. Huang, X. Duan, and C. M. Lieber, "Nanowires for integrated multicolor nanophotonics," *Small* **1**(1), 142-147 (2005) [[doi:10.1002/sml.200400030](https://doi.org/10.1002/sml.200400030)].
- [7] Y. Cui, Q. Wei, H. Park, and C. M. Lieber, "Nanowire nanosensors for highly sensitive and selective detection of biological and chemical species," *Science* **293**(5533), 1289-1292 (2001) [[doi:10.1126/science.1062711](https://doi.org/10.1126/science.1062711)].
- [8] J. B. Baxter and E. S. Aydil, "Nanowire-based dye-sensitized solar cells," *Appl. Phys. Lett.* **86**(5), 053114 (2005) [[doi:10.1063/1.1861510](https://doi.org/10.1063/1.1861510)].
- [9] J. Qi, A. M. Belcher, and J. M. White, "Spectroscopy of individual silicon nanowires," *Appl. Phys. Lett.* **82**(16), 2616-2618 (2003) [[doi:10.1063/1.1569982](https://doi.org/10.1063/1.1569982)].
- [10] J. -Q. Xi, J. K. Kim, and E. F. Schubert, "Silica nanorod-array films with very low refractive indices," *Nano Lett.* **5**(7), 1385-1387 (2005) [[doi:10.1021/nl050698k](https://doi.org/10.1021/nl050698k)].
- [11] Y. Wang, K. Kempa, B. Kimball, J. B. Carlson, G. Benham, W. Z. Li, T. Kempa, J. Rybczynski, A. Herczynski, and Z. F. Ren, "Receiving and transmitting light-like radio waves: Antenna effect in arrays of aligned carbon nanotubes," *Appl. Phys. Lett.* **85**(13), 2607-2609 (2004) [[doi:10.1063/1.1797559](https://doi.org/10.1063/1.1797559)].
- [12] K. Hadobas, S. Kirsch, A. Carl, M. Acet, and E. F. Wassermann, "Reflection properties of nanostructure-arrayed silicon surfaces," *Nanotech.* **11**(3), 161-164 (2000) [[doi:10.1088/0957-4484/11/3/304](https://doi.org/10.1088/0957-4484/11/3/304)].
- [13] C. Lee, S. Y. Bae, S. Mobasser, and H. Manohara, "A novel silicon nanotips antireflection surface for the Micro Sun Sensor," *Nano. Lett.* **5**(12), 2438-2442 (2005) [[doi:10.1021/nl0517161](https://doi.org/10.1021/nl0517161)].
- [14] S. Koynov, M. S. Brandt, and M. Stutzmann, "Black nonreflecting silicon surfaces for solar cells," *Appl. Phys. Lett.* **88**(20), 203107 (2006) [[doi:10.1063/1.2204573](https://doi.org/10.1063/1.2204573)].
- [15] L. L. Ma, Y. C. Zhou, N. Jiang, X. Lu, J. Shao, W. Lu, J. Ge, X. M. Ding, and X. Y. Hou, "Wide-band "black silicon" based on porous silicon," *Appl. Phys. Lett.* **88**(17), 171907 (2006) [[doi:10.1063/1.2199593](https://doi.org/10.1063/1.2199593)].
- [16] A. V. Shah, M. Vanecek, J. Meier, F. Meillaud, J. Guillet, D. Fischer, C. Droz, X. Niquille, S. Fay, E. Vallat-Sauvain, V. Terrazzoni-Daudrix, and J. Bailat, "Basic efficiency limits, recent experimental results and novel light-trapping schemes in a-Si:H, lc-Si:H and 'micromorph tandem' solar cells," *J. Non-Cryst. Sol.* **338-340**(1), 639-645 (2004) [[doi:10.1016/j.jnoncrsol.2004.03.074](https://doi.org/10.1016/j.jnoncrsol.2004.03.074)].
- [17] R. A. Myers, R. Farrell, A. Karger, J. E. Carey, and E. Mazur, "Enhancing near-infrared avalanche photodiode performance by femtosecond laser microstructuring," *Appl. Opt.* **45**(35), 8825-8831 (2006) [[doi:10.1364/AO.45.008825](https://doi.org/10.1364/AO.45.008825)].

- [18] K. Q. Peng, Z. P. Huang, and J. Zhu, "Fabrication of large-area silicon nanowire p-n junction diode arrays," *Adv. Mater.* **16**(1), 73-76 (2004) [[doi:10.1002/adma.200306185](https://doi.org/10.1002/adma.200306185)].
- [19] R. S. Wagner and W. C. Ellis, "Vapor-liquid-solid mechanism of single crystal growth," *Appl. Phys. Lett.* **4**(5), 89-90 (1964) [[doi:10.1063/1.1753975](https://doi.org/10.1063/1.1753975)].
- [20] J. Rappich, S. Lust, I. Sieber, W. Henrion, J. K. Dohrmann, W. Fuhs, "Light trapping by formation of nanometer diameter wire-like structures on  $\mu\text{c-Si}$  thin films," *J. Non-Cryst. Sol.* **266-269**(1), 284-289 (2000)[[doi:10.1016/S0022-3093\(99\)00837-6](https://doi.org/10.1016/S0022-3093(99)00837-6)].
- [21] J. -Q. Xi, M. F. Schubert, J. K. Kim, E. F. Schubert, M. Chen, S. -Y. Lin, W. Liu , and J. A. Smart, "Optical thin-film materials with low refractive index for broadband elimination of Fresnel reflection," *Nature Photon.* **1**(3), 176-179 (2007) [[doi:10.1038/nphoton.2007.26](https://doi.org/10.1038/nphoton.2007.26)].
- [22] M. B. Robinson, A. C. Dillon, D. FL. Haynes, and S. M. George, "Effect of thermal annealing and surface coverage on porous silicon photoluminescence," *Appl. Phys. Lett.* **61**(12), 1414-1416 (1992) [[doi:10.1063/1.107555](https://doi.org/10.1063/1.107555)].
- [23] C. Wu, C. H. Crouch, L. Zhao, and J. E. Carey, R. Younkin, J. A. Levinson, E. Mazur, R. M. Farrell, P. Gothoskar, and A. Karger, "Near-unity below-band-gap absorption by microstructured silicon," *Appl. Phys. Lett.* **78**(13), 1850-1852 (2001) [[doi:10.1063/1.1358846](https://doi.org/10.1063/1.1358846)].
- [24] E. Yablonovitch and G. D. Cody, "Intensity enhancement in textured optical sheets for solar cells," *IEEE Trans. Electron. Dev.* **29**, 300-305 (1982).
- [25] P. B. Clapham and M. C. Hutley, "Reduction of lens reflexion by the "Moth Eye" principle," *Nature* **244**(5414), 281-282 (1973) [[doi:10.1038/244281a0](https://doi.org/10.1038/244281a0)].
- [26] S. J. Wilson and M. C. Hutley, "The optical properties of 'moth eye' antireflection surfaces," *Opt. Acta* **29**(7), 993-1009 (1982).
- [27] H. Seel and R. Brendel, "Optical absorption in crystalline Si films containing spherical voids for internal light scattering," *Thin Solid Films* **451-452**, 608-611 (2004) [[doi:10.1016/j.tsf.2003.11.049](https://doi.org/10.1016/j.tsf.2003.11.049)].
- [28] S. T. Chu and S. K. Chaudhuri, "A finite-difference time-domain method for the design and analysis of guided-wave optical structures," *J. Lightwave Technol.* **7**, 2033-2038 (1989) [[doi:10.1109/50.41625](https://doi.org/10.1109/50.41625)].
- [29] C. F. Bohren and D. R. Huffman, *Absorption and Scattering of Light by Small Particles*, Wiley-Interscience, New York (1983).
- [30] J. Lee, A. O. Govorov, J. Dulka, and A. N. Kotov, "Bioconjugates of CdTe nanowires and Au nanoparticles: Plasmon-exciton interactions, luminescence enhancement, and collective effects," *Nano. Lett.* **4**(12), 2323-2330 (2004) [[doi:10.1021/nl048669h](https://doi.org/10.1021/nl048669h)].
- [31] J. R. Cole and N. J. Halas, "Optimized plasmonic nanoparticle distributions for solar spectrum harvesting," *Appl. Phys. Lett.* **89**(15), 153120 (2006) [[doi:10.1063/1.2360918](https://doi.org/10.1063/1.2360918)].